

Evidence for planar pinning in heavily Pb-substituted $\text{Bi}_2\text{Sr}_2\text{CaCu}_2\text{O}_{8+y}$ single crystals

K. Itaka, H. Taoka, S. Ooi, T. Shibauchi,* and T. Tamegai

Department of Applied Physics, The University of Tokyo, 7-3-1 Hongo, Bunkyo-ku, Tokyo 113-8656, Japan

(Received 13 May 1999)

We studied the vortex pinning properties in $\text{Bi}_{2.2-x}\text{Pb}_x\text{Sr}_{1.8}\text{CaCu}_2\text{O}_{8+y}$ ($0 \leq x \leq 0.6$) single crystals, with and without laminar microstructures (LM's) parallel to the a axis. We found a large and temperature-dependent in-plane anisotropy in the critical current density (J_c) in the case of $x=0.6$ with LM's. Magnetization under various field directions was measured using micro-Hall probes. J_c , when the field is tilted within the LM's, is larger than that when the field is tilted away from the LM's. This strongly supports that LM's act as planar pinning centers in this system. We also found a crossover from fishtail-like behavior to second-peak-like behavior when the field is tilted more than 70° from the c axis. [S0163-1829(99)50938-7]

Among many high-temperature superconductors, $\text{Bi}_2\text{Sr}_2\text{CaCu}_2\text{O}_{8+y}$ (BSCCO) has been considered one of the most promising materials for applications. It has great advantage for synthesis of superconducting wires with a strongly grain-aligned microstructure. However, the critical current density (J_c) of BSCCO is very small in spite of a high critical temperature (T_c). There are mainly two reasons for a small J_c in BSCCO. The first one is the large electronic anisotropy. In layered superconductors, the vortices are influenced by thermal fluctuations and the dissipation reduces J_c . When the anisotropy of the sample is increased by the reduction of carrier density, J_c will decrease because the line tension of the vortex becomes smaller.¹ The second one is the absence of effective pinning centers. Oxygen vacancies or impurities act as pointlike pinning centers,² but the pinning force is not enough to achieve a large J_c . On the other hand, columnar defects in a heavy-ion irradiated sample act as linelike pinning centers and cause a large enhancement of J_c (Refs. 3–5). Such a correlated disorder has a higher pinning efficiency. Although heavy-ion irradiation is an effective way to introduce pinning centers in the sample, it is not of industrial use. On the other hand, an alternative method for the introduction of defects is chemical substitution. For example, the substitution of Pb for Bi sites was tried, but the enhancement of J_c is small, especially above 30 K, because the defects are random point pinning centers.^{6–9} Recently, however, in heavily Pb-substituted BSCCO $\text{Bi}_{2.2-x}\text{Pb}_x\text{Sr}_{1.8}\text{CaCu}_2\text{O}_{8+y}$ (BPSCCO), remarkable increases in J_c and irreversibility temperature (T_{irr}) were observed.¹⁰ When $x \geq 0.6$ in BPSCCO, J_c increases dramatically, espe-

cially in high temperature regions above 40 K. In this system, there are alternating laminar microstructures (LM's), which consist of Pb-rich and Pb-poor regions. The origin of LM's is related with eutectics and eutectoids using the floating zone (FZ) method.¹¹ LM's are believed to be the effective pinning centers and cause the enhancement of J_c and the irreversibility line. One of the evidences for this is the fact that annealing the sample at 816°C destroys LM's and decreases J_c in a certain field region.¹² However, the detailed nature of LM's as pinning centers remains to be clarified. It is interesting to ask which is the origin of a large enhancement of J_c , the strength of the pinning potential by LM's or the geometrical form of them. In this paper, we studied the nature of LM's as pinning centers using a magneto-optical method and micro-Hall probes.

Single crystals of $\text{Bi}_{2.1}\text{Sr}_{1.9}\text{CaCu}_2\text{O}_{8+y}$ (BSCCO) and $\text{Bi}_{2.2-x}\text{Pb}_x\text{Sr}_{1.8}\text{CaCu}_2\text{O}_{8+y}$ ($x=0.2,0.4,0.6$) (BPSCCO) have been grown by the floating zone method in air with a crystal growth speed of 0.5 mm/h (Refs. 10–12). The characteristics of the crystals used in the present study are summarized in Table I. The final content of Pb in the sample was checked by using inductively coupled plasma (ICP) chemical analysis. The Pb content was always smaller than the starting composition, because Pb evaporates during the crystal growth. We used only as-grown crystals because the LM's disappear by annealing. We checked the presence of the LM's using a transmission electron microscope (TEM) in a piece next to the crystal which was used in the magnetic measurements. The inset in Fig. 1 shows a typical TEM image of the sample with LM's, with the incident electron

TABLE I. Characteristics of samples and in-plane anisotropy of J_c . The final content of Pb and Bi is determined using ICP analysis assuming the Cu content is 2.00

Sample	Pb content x (start/final)	Bi content (start/final)	laminar structures (TEM)	T_c (K)	J_c^a/J_c^b
2C-1	0.2/0.13	2.00/1.94	×	82	1.0 (18 K~26 K)
4C-1	0.4/0.29	1.80/1.77	×	80	1.0 (10 K~18 K)
6B-1	0.6/0.34	1.60/1.70	×	78	1.2 (12 K~19 K)
6G-2	0.6/0.27	1.60/1.60	○	70	1.4 (8 K)~3.5(40 K)
6G-3	0.6/0.27	1.60/1.60	○	72	1.2 (14 K)~3.0(30 K)
BSCCO			×	89	0.94 (18 K~26 K)

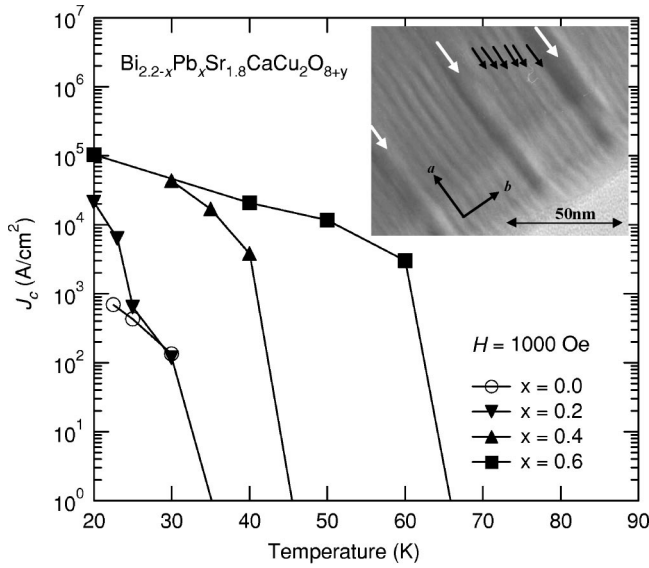


FIG. 1. Comparison of the temperature dependence of J_c for BPSCCO with different Pb content at $H=1$ kOe. (inset) Typical TEM image for BPSCCO ($x=0.6$) with LM's with incident beams parallel to the c axis. The larger stripes (white arrows) are LM's and the smaller ones (black arrows) correspond to the lattice modulation along the b axis.

beams parallel to the c axis. The LM's run along the a axis and the distance between them is about 500 \AA . The region between the LM's has lattice modulation along the b axis as in pure BSCCO. The LM's have no lattice modulation, and the thickness is about 100 \AA . These results are similar to that reported in Ref. 10. The single crystals were cut into typical dimensions of $0.5 \times 0.5 \times 0.05 \text{ mm}^3$ before measuring T_c and J_c by using a commercial superconducting quantum interference device (SQUID) magnetometer (MPMS-XL5, Quantum Design) with the applied field H parallel to the c axis. The main panel of Fig. 1 shows the temperature dependence of J_c in our crystals. We estimated J_c using the Bean model.¹³ In this model, irreversible magnetization, $M_{irr} = (M_{dec} - M_{inc})/2$ [G], is related to J_c [A/cm²] as $J_c = 40M_{irr}/r$, where r [cm] is the radius of the circulating current which we assumed to be the lateral dimension of the crystal. The T_c of our samples are about 15 K lower than that reported in Ref. 11, probably due to different cation stoichiometry and/or oxygen content. The temperature dependence of J_c at $H=1$ kOe measured for the sample with $x \geq 0.6$ is dramatically different from that for the sample with $x \leq 0.4$, especially above 40 K. This behavior is in good agreement with the data in Ref. 11, although the values of J_c are smaller by a factor of 5. Considering the large J_c of about 10^4 A/cm^2 even at 50 K, the LM's are not considered to behave like weak links which limits the current flow across them.

In-plane anisotropy of $J_c (=J_c^a/J_c^b)$ was investigated by observing the critical state field profile using magneto-optical indicator garnet film.¹⁴ We also measured the M - B hysteresis curves for the c -axis component as functions of applied field using micro-Hall probes with two active elements.

The inset in Fig. 2 shows a typical critical state field profile in BPSCCO ($x=0.6$, 6G-2) with the LM's. We defined the current discontinuity line from the dark region in this

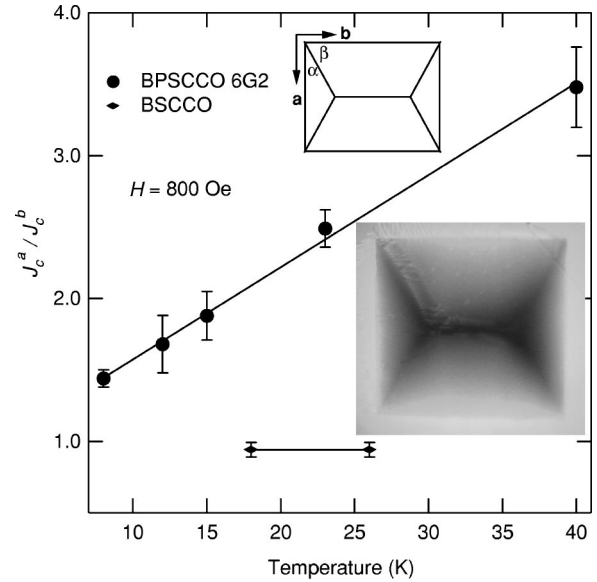


FIG. 2. Temperature dependence of J_c^a/J_c^b in BPSCCO with LM's at $H=800$ Oe. In a pure BSCCO, J_c^a/J_c^b is almost unity. The inset shows the critical state field profile at 15 K for the sample 6G-2 using a magneto-optical technique. We estimate the anisotropy of $J_c (=J_c^a/J_c^b)$ from the current discontinuity line (see text).

image and defined angles α and β .^{15,16} The in-plane anisotropy of J_c is estimated to be 1.7 using the relation $J_c^a/J_c^b = \sin \beta / \sin \alpha$. The value of J_c^a/J_c^b varies from 1.4 to 3.5 in the temperature region between 8 and 40 K. The main panel of Fig. 2 shows the temperature dependence of J_c^a/J_c^b in the sample with LM's. J_c^a/J_c^b increases almost linearly as temperature increases. On the other hand, in the samples near the crystal without LM's, J_c^a/J_c^b is almost unity. In the crystal without LM's, the value of J_c^a/J_c^b is a little larger than that in a pure BSCCO. In a pure BSCCO, J_c^a/J_c^b is 0.94 ± 0.05 (Ref. 17). The anisotropy in J_c is understood as follows: Because the LM's run parallel to the a axis and are believed to be pinning centers, the vortex cannot easily move along the b axis and hence increases J_c^a relative to J_c^b . It is clearly seen in Table I that only crystals which are inferred to have LM's show large and temperature-dependent anisotropy of in-plane J_c . At low temperatures, pinning by point defects becomes more dominant than pinning by LM's; hence the anisotropy in J_c becomes smaller. J_c^a/J_c^b is also related to the in-plane anisotropy of coherence length. In an untwined $\text{YBa}_2\text{Cu}_3\text{O}_{7-y}$ (YBCO) single crystal, the value of J_c^a/J_c^b is explained by the in-plane anisotropy of coherence length.¹⁵ In this case, the value of J_c^a/J_c^b does not reveal the property of the pinning centers. In BPSCCO with LM's, a large in-plane anisotropy of coherence lengths is not expected, but this point needs clarification.

To investigate the relation between in-plane anisotropic pinning centers and the enhancement of J_c , we measured local magnetization under tilted applied fields using micro-Hall-probes. In the rest of this paper, we show data only for sample 6G-2 with LM's. Figures 3(a) and 3(b) show hysteresis curves of a magnetization along the c axis as a function of magnetic induction along the c axis. We defined φ as the angle between the projection of the field to the ab plane and the plane of LM's. The field is tilted by θ from the c axis

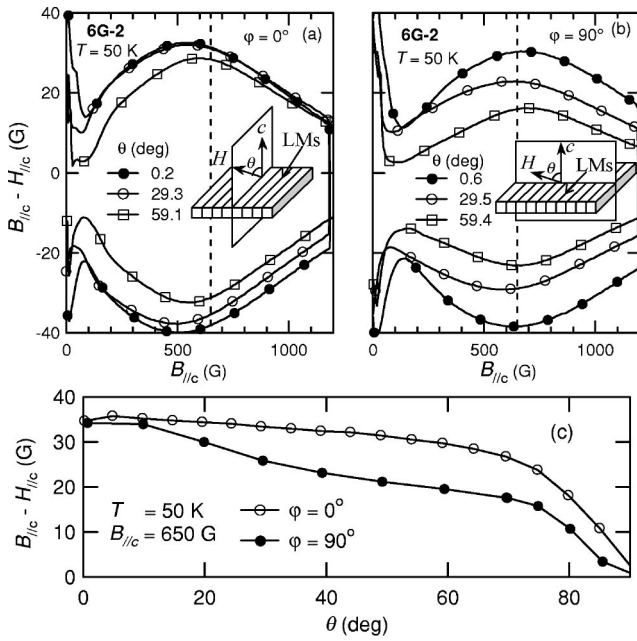


FIG. 3. M - B hysteresis curves at 50 K for the sample 6G-2. The applied field is tilted from the c axis (a) parallel to the LM's ($\varphi = 0^\circ$), or (b) perpendicular to the LM's ($\varphi = 90^\circ$). (c) The angular dependence of the irreversible magnetization at $H = 620$ Oe [dashed lines in (a) and (b)]. When $\theta \leq 10^\circ$, the difference between $\varphi = 0^\circ$ and $\varphi = 90^\circ$ is small.

towards the a and b axes in Figs. 3(a) and 3(b), respectively. In the case of $\theta = 0$, in two kinds of φ configurations, the M - B curve should be the same. A small difference between the two configurations is due to the repositioning of the sample. When $\varphi = 0^\circ$, the field direction is always within the LM's. In this case, the M - B curves do not change so much below $\theta = 60^\circ$. On the other hand, when $\varphi = 90^\circ$, the magnetization decreases more rapidly when θ is increased. To make the difference clearer, we plot the angular dependence of the irreversible magnetization near the fishtail-like peak in Fig. 3(c). In pure BSCCO, when the field is tilted, the magnetization is almost constant or increases slightly,^{18,19} whereas in this system the magnetization depends remarkably on the direction of the applied field. We consider that this difference originates from the pinning property of the LM's. When θ is above 75° , the difference between $\varphi = 0^\circ$ and 90° becomes smaller because the pinning properties of vortices are determined by the presence of CuO_2 planes rather than LM's.

Figure 4 shows the comparison of irreversible magnetization (M_{irr}) as a function of the c -axis component of the field for $\varphi = 0^\circ$ and $\varphi = 90^\circ$ with the same value of θ at 50 K. In order to make a proper comparison between the data for $\varphi = 0^\circ$ and $\varphi = 90^\circ$, we normalized M_{irr} by the broad peak value at around $H = 600$ Oe at $\theta = 0^\circ$ for the two kinds of settings. M_{irr} for $\varphi = 0^\circ$ is always larger than that for $\varphi = 90^\circ$. If we assume a simple summation of pinning forces, the arrows in the figure show the contribution from the LM's. The enhancement of M_{irr} caused by the LM's becomes appreciable above $H = 100$ Oe and has a broad maximum at around $H = 500$ Oe. If the LM's extend to the sample edge, J_c is expected to decrease in a certain range of field due to the channeling of vortices along the LM's. Ac-

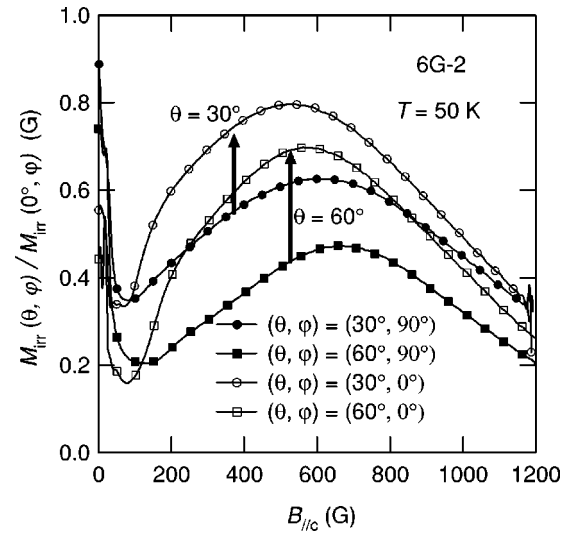


FIG. 4. Comparison of normalized irreversible magnetization between $\varphi = 0^\circ$ and $\varphi = 90^\circ$ at $T = 50$ K. The open symbols show data when the field is tilted parallel to the LM's. The closed symbols show data when the field is tilted perpendicular to the LM's. The arrows show the difference in M_{irr} between $\varphi = 0^\circ$ and $\varphi = 90^\circ$ with the same θ values.

tually, such a suppression of irreversible magnetization due to the channeling of vortices along the twin boundaries is reported in YBCO (Ref. 20). However, the present sample does not show such a behavior.²¹ This suggests that the LM's do not extend to the sample edge but have finite dimension along the a axis, consistent with the TEM observation by Hiroi *et al.*¹¹ In this case, the LM's are analogous to the columnar defects, although the shape is highly anisotropic. If we assume the extension of the LM's along the a axis to be $1 \mu\text{m}$, and use the observed separation of the LM's along the b axis, the "matching field" is estimated as 400 G,

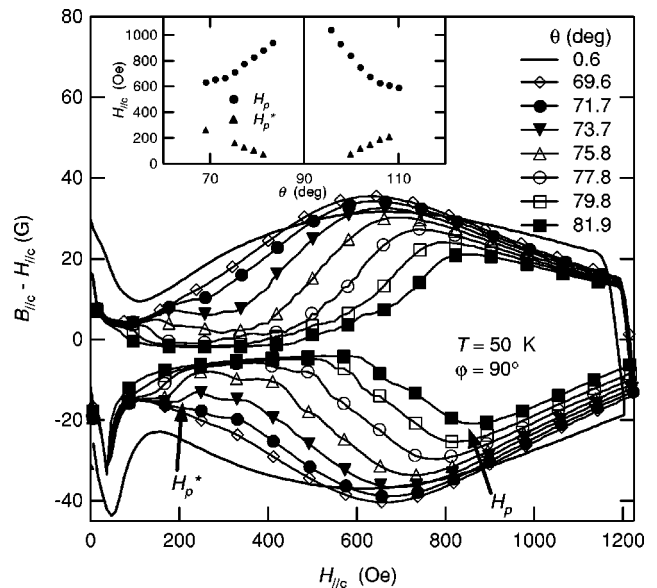


FIG. 5. M - H hysteresis curves at 50 K for the sample 6G-2 at large θ in the case of $\varphi = 90^\circ$. The broad fishtail-like peak crosses over to the second-peak-like structure for $\theta \geq 70^\circ$. In the same angle range, a new anomaly is observed at $H_p^* < H_p$. The inset shows the angular dependence of H_p and H_p^* in BPSCCO.

which is close to the field value where we have the maximum increase in J_c . A matching effect in this case would not be sharp because there is a large distribution of the size and the separation of the LM's. Usually, the matching field is temperature independent, because it is determined by the geometrical configuration of pinning sites. However, the "matching field" in the present case can increase at lower temperature, because the trapping capability of vortices (the average number of vortices trapped in a piece of a LM) would increase at lower temperatures due to the increase in the pinning potential. This scenario is consistent with our findings.

These results indicate that in-plane anisotropic pinning centers exist and cause the enhancement of J_c in BPSCCO with LM's. We ascribe all these features to the presence of LM's.

Figure 5 shows M - H curves at larger θ in BPSCCO with $x=0.6$. Below $\theta=70^\circ$, there is a broad maximum in M - H curves which look like fishtail effects in YBCO.² Above $\theta=70^\circ$, magnetization at the intermediate field region is rapidly suppressed and the hysteresis curves become wavy. At the same time a new anomaly appears at the low field, which we designate as H_p^* . Interestingly, the shape of the M - H hysteresis loop becomes very similar to what we observe in overdoped BSCCO without Pb.²² The peak at the higher field becomes more like the second peak rather than the fishtail peak. This crossover in the shape of the M - H curve and the appearance of H_p^* occur above $\theta=70^\circ$ irrespective of the value of φ . The origin of H_p^* could be the instability of the

triangular vortex lattice in highly anisotropic superconductors in tilted fields²³ or structural phase transition in the vortex lattice which accompanies the generation of a chainlike structure.²⁴ The second peak effect is rather ubiquitous in BSCCO, and we suppose that the pronounced fishtail effect in Pb doped crystal makes it difficult to observe the second peak effect. By suppressing the fishtail peak, the second peak becomes visible at large θ . The mechanism of the suppression of the fishtail peak is not clear at present. However, it is for sure that the presence of the in-plane field has intimate relation to this crossover. Conversely, the study of this suppression of the fishtail effect may shed some light on the mechanism of the fishtail effect itself.

We investigated the vortex states in $\text{Bi}_{2.2-x}\text{Pb}_x\text{Sr}_{1.8}\text{CaCu}_2\text{O}_{8+y}$ ($0 \leq x \leq 0.6$) single crystals, with and without LM's. Using a magneto-optical technique, we found a large and temperature-dependent in-plane anisotropy of critical current density in $x=0.6$ with LM's. The M - B curve for fields tilted from the c axis perpendicular to the LM's is different from that tilted parallel to the LM's. The LM's act as planar pinning centers in a wide region ($\theta=0 \sim 70^\circ$, $B_{//c}=100 \sim 1000$ G) and cause the large enhancement of J_c . When $\theta \geq 70^\circ$, the M - B curves crossover from fishtail-like behavior to second-peak-like behavior.

We thank M. Ichihara for the TEM observations. This work is supported in part by CREST and Grant-in-Aid for Scientific Research from the Ministry of Education, Science, Sports and Culture, Japan.

*Present address: IBM T. J. Watson Research Center, Yorktown Heights, NY 10548 and MST-STC, Los Alamos National Laboratory, MS-K763, Los Alamos, NM 87545.

¹G. Blatter *et al.*, Rev. Mod. Phys. **66**, 1125 (1994).

²M. Daeumling *et al.*, Nature (London) **346**, 332 (1990).

³L. Civale *et al.*, Phys. Rev. Lett. **67**, 648 (1991).

⁴M. Konczykowski *et al.*, Phys. Rev. B **44**, 7167 (1991).

⁵L. Civale, Supercond. Sci. Technol. **10**, A11 (1997).

⁶Y. L. Wang *et al.*, Proc. Natl. Acad. Sci. USA **87**, 7058 (1990).

⁷N. Fukushima *et al.*, Physica C **159**, 777 (1989).

⁸P. Fourier *et al.*, Physica C **257**, 291 (1996).

⁹Y. Yamaguchi *et al.*, *Advances in Superconductivity* (Springer-Verlag, Tokyo, 1996), Vol. VIII, p. 231.

¹⁰I. Chong *et al.*, Science **276**, 770 (1997).

¹¹Z. Hiroi *et al.*, J. Solid State Chem. **138**, 98 (1998).

¹²Z. Hiroi *et al.*, *Advances in Superconductivity* (Springer-Verlag, Tokyo, 1998), Vol. X, p. 285.

¹³C. P. Bean, Rev. Mod. Phys. **36**, 31 (1964).

¹⁴A. Forkl and H. Kronmüller, Phys. Rev. B **52**, 16 130 (1995).

¹⁵T. Tamegai *et al.*, *Critical Currents in Superconductors* (World Scientific, Singapore, 1996), p. 125.

¹⁶T. Haage *et al.*, Phys. Rev. B **56**, 8404 (1997).

¹⁷H. Taoka *et al.* (unpublished).

¹⁸Y. Yamaguchi *et al.*, Physica C **273**, 261 (1997).

¹⁹S. Ooi *et al.*, *Advances in Superconductivity* (Springer-Verlag, Tokyo, 1998), Vol. X, p. 465.

²⁰M. Oussena *et al.*, Phys. Rev. B **51**, 1389 (1995).

²¹In some of the crystals, we observed a suppression of J_c in a limited field region, which can be considered as a sign of channeling effect. The different behavior among crystals with LM's can be understood by considering the different degree of the continuity of LM's along the plane.

²²S. Ooi *et al.*, Physica C **302**, 339 (1998).

²³A. M. Thompson and M. A. Moore, Phys. Rev. B **55**, 3856 (1997).

²⁴A. E. Koshelev, Phys. Rev. Lett. **83**, 187 (1999).